Heme Oxygenase 1 in Schwann Cells Regulates Peripheral Nerve Degeneration Against Oxidative Stress

Muwoong Kim[1], Hyosun Kim[1,2], Dogyeong Kim[1,2], Dokyoung Kim[1,2], Youngbuhm Huh[1,2], Chan Park[1,2], Hyung-Joo Chung[3], Junyang Jung[1,2] (ID) and Na Young Jeong[4]

Abstract

During Wallerian degeneration, Schwann cells lose their characteristic of myelinating axons and shift into the state of developmental promyelinating cells. This recharacterized Schwann cell guides newly regrowing axons to their destination and remyelinates reinnervated axons. This Schwann cell dynamics during Wallerian degeneration is associated with oxidative events. Heme oxygenases (HOs) are involved in the oxidative degradation of heme into biliverdin/bilirubin, ferrous iron, and carbon monoxide. Overproduction of ferrous iron by HOs increases reactive oxygen species, which have deleterious effects on living cells. Thus, the key molecule for understanding the exact mechanism of Wallerian degeneration in the peripheral nervous system is likely related to oxidative stress-mediated HOs in Schwann cells. In this study, we demonstrate that demyelinating Schwann cells during Wallerian degeneration highly express HO1, not HO2, and remyelinating Schwann cells during nerve regeneration decrease HO1 activation to levels similar to those in normal myelinating Schwann cells. In addition, HO1 activation during Wallerian degeneration regulates several critical phenotypes of recharacterized repair Schwann cells, such as demyelination, transdedifferentiation, and proliferation. Thus, these results suggest that oxidative stress in Schwann cells after peripheral nerve injury may be regulated by HO1 activation during Wallerian degeneration and oxidative-stress-related HO1 activation in Schwann cells may be helpful to study deeply molecular mechanism of Wallerian degeneration.

Keywords

Introduction

After peripheral nerve injury, Schwann cells play unique roles in peripheral nerves. Denervating signals induce intracellular events in mature Schwann cells and the myelin sheath in Schwann cells is then broken down molecularly and mechanically by recruited macrophages and the Schwann cells themselves. Besides myelin fragmentation, at the distal part of the peripheral nerve after injury, axonal degradation occurs directly by the axons themselves (Fischer et al., 2012; Bros et al., 2014)) and indirectly by Schwann cells (Jung et al., 2011a). These phenomena are known as Wallerian degeneration. Efficient Wallerian degeneration leads to efficient peripheral nerve regeneration. However, once in a while, under

[1]Department of Anatomy and Neurobiology, College of Medicine, Kyung Hee University, Seoul, Korea
[2]Department of Biomedical Science, Medical Research Center for Bioreaction to Reactive Oxygen Species and Biomedical Science Institute, Graduation School, Kyung Hee Univeristy, Seoul, Korea
[3]Department of Anesthesiology and Pain Medicine, College of Medicine, Kosin University, Busan, Korea
[4]Department of Anatomy and Cell Biology, College of Medicine, Dong-A University, Busan, Korea

Corresponding Authors:
Junyang Jung, Department of Anatomy and Neurobiology, College of Medicine, Kyung Hee Univeristy, 26, Kyungheedae-ro, Dongdaemun-gu, Seoul 02447, Korea.
Email: jjung@khu.ac.kr
Na Young Jeong, Department of Anatomy and Cell Biology, College of Medicine, Dong-A Univeristy, 32, Daesingongwon-ro, Seo-gu, Busan 49201, Korea.
Email: jnyjjy@dau.ac.kr

acute abnormal conditions, such as mechanical injury of peripheral nerves, the nerve degeneration becomes inefficient and the degenerated peripheral nerve is not recovered or regenerated. One of the causes of entry into a neurodegenerative state is oxidative stress (D'Aguanno et al., 2010; Caillaud et al., 2018).

Heme oxygenases (HOs) consist of two isoforms, HO1 (heat-shock protein 32) and HO2, which catalyze the oxidation of cellular heme into biliverdin, ferrous iron, and carbon monoxide (CO) in mammalian cells. HOs are well studied in the central nervous system. In normal brain, HO2 is widely and abundantly distributed in neuronal and nonneuronal cells throughout the brain and spinal cord (Verma et al., 1993; Dwyer et al., 1995). In contrast, HO1 is not expressed in normal, unstressed brain, but is highly expressed in stressed brain (Maines, 1997; Platt and Nath, 1998). For example, HO1 is highly expressed in glial cells in brain neurodegenerative diseases, such as Alzheimer's disease and Parkinson's disease (Schipper et al., 1995, 1998). In the peripheral nervous system (PNS), HO1 is highly expressed in Schwann cells of sciatic nerves after nerve injury (Hirata et al., 2000; Yama et al., 2016). These studies imply that HO1 activation is related to oxidative stress-mediated nerve degeneration; however, the authors did not determine, in detail, the oxidative stress-mediated molecular, functional, or morphological mechanisms by which Schwann cells via HO1 activation guide Wallerian degeneration and nerve regeneration in injured Schwann cells.

Here, using *in vitro*, *ex vivo*, and *in vivo* peripheral neurodegenerative models, we show the HO1 activation pattern in Schwann cells during peripheral nerve degeneration and regeneration and demonstrate that regulation of HO1 in Schwann cells affects critical events in Wallerian degeneration such as demyelination, and Schwann cell transdedifferentiation and proliferation. Our results indicate that the regulation of HO1 activation in Schwann cells likely protects against oxidative stress-induced neural damage and that HO1 represents an effective therapeutic target for peripheral nerve degenerative diseases.

Material and Methods

Animals

Adult male Sprague-Dawely rats (RRID:RGD_7246927; 200 g, Samtako, Osan, Korea) were used for all *in vitro*, *ex vivo*, and *in vivo* experiments. All experiments were conducted according to protocols approved by the Kyung Hee University Committee on Animal Research, KHUASP(SE)-16-043-1, following the guidelines of animal experimentation established by the Korean Academy of Medical Sciences.

Materials

All antibodies were commercially purchased and used for immunochemistry or Western blotting. Antibodies against HO1 (RRID:AB_10618757) and HO2 (RRID: AB_11180908) were from Enzo Life Sciences Inc. (Farmigdale, NY, USA). Antibodies against myelin basic protein (MBP, RRID:AB_92396), lysosomal-associated membrane protein 1 (LAMP1, RRID: AB_2134495), p75 nerve growth factor receptor (p75, RRID:AB_2267254), and nitric oxide synthase 1 (NOS1, RRID:AB_2152494) were from Santa Cruz Biotechnology (Santa Cruz, CA, USA). Anti-Ki67 (RRID:AB_302459) was from Abcam (Cambridge, UK). Neurofilament (NF, RRID:AB_94275) and Alexa Fluor 488- and 594-conjugated secondary antibodies (488-, RRID:AB_141607; 594-, RRID:AB_2534105, 141637, 2535795) were from Life Technologies (Grand Island, NY, USA). Nrg1 (human NRG1-β1 extracellular domain) and forskolin were obtained from R&D Systems (Minneapolis, MN, USA) and Calbiochem (Gibbstown, NJ, USA), respectively. All of the other antibodies (β-actin, RRID:AB_476744; S100β, RRID:AB_477499) and HO-inhibitory drugs were obtained from Sigma-Aldrich (St. Louis, MO, USA).

Explant Culture

Ex vivo sciatic nerve explant cultures were conducted as previously described (Park et al., 2015). Briefly, the sciatic nerves are extracted and connective tissues around the sciatic nerves were removed under a stereomicroscope. The extracted sciatic nerves were divided into 3 to 4 mm small size pieces in length. For sciatic nerve explant culture, the nerve pieces were incubated in Dulbecco's Modified Eagle's Medium (DMEM) containing 10% fetal bovine serum (FBS), L-glutamine (4 mM), penicillin (100 U/mL), and streptomycin (100 μg/mL) at 37°C in a humidified atmosphere of 5% CO_2. Before treating the explant culture with HO1-inhibitory drugs, the culture medium was replaced with DMEM containing 2% FBS. The sciatic explants were cultured for 3 days and used for immunostaining analysis or Western blot analysis.

Primary Schwann Cell culture and CO Probe Staining

Primary Schwann cells were isolated from the sciatic nerves of adult rats as we previously described (Shin et al., 2012). Briefly, the extracted sciatic nerves were digested by collagenase (2 mg/mL) in calcium/magnesium-free Hank's buffered solution at 37°C for 20 min, and then, the nerves were treated with 0.05% trypsin at 37°C for 10 min. The chemically digested nerves were dissociated into cell pellets using a flame-polished Pasteur pipette. To increase the Schwann cell

population, cells were kept in DMEM containing 1% FBS, Nrg1 (30 ng/mL), and forskolin (5 μM) for 2 to 4 generations. For CO staining, CO-specific fluorescent probes (Michel et al., 2012) were concentration dependently (0, 0.1, 1, and 10 μM) added to the primary Schwann cells without Nrg1 treatment and then left for 30 min.

Calculation of Myelin-Related Indices

To verify morphologically the degree of myelin fragmentation during Wallerian degeneration, we used ovoid index and myelin index. Calculating myelin-related indices was performed as described previously (Jung et al., 2011a; Park et al., 2015). Ovoid index is the number of myelin ovoids within 200 μm of a teased nerve fiber under a differential interference contrast (DIC)-filtered microscope. In a bar graph, Index 1 is equivalent to one ovoid on a teased nerve fiber. Myelin index shows the number of nerve fibers which contain intact myelin sheaths with longer than 50 μm among 100 teased nerve fibers under a microscopic field. In a graph, Index 1 is equivalent to one nerve fiber including 50-μm-long intact myelin. Based on our experimental experience, we established a standard (size of ovoid = 200 μm; length of double lines of MBP stain = 50 μm).

Immunostaining

For immunostaining, primary Schwann cells, frozen nerve sections, and teased nerve fibers were prepared. First, to obtain teased nerve fibers, *ex vivo*, *in vivo* sciatic nerve segments were incubated for 1 day in 4% para-formaldehyde at 4°C. The nerve sheath was removed, and the segments were separated into one single fiber using fine forceps. Primary Schwann cells, teased nerve fibers, and frozen nerve sections on slides were postfixed in 4% para-formaldehyde for 15 min at room temperature (RT). The sample slides were blocked by preincubation with 1% bovine serum albumin in phosphate-buffered saline (PBS) at RT for 1 hr. The slides were incubated with primary antibodies in PBS overnight at 4°C and then with secondary antibodies in PBS for 2 hr at RT. To identify the nucleus of the cells, the slides were counterstained with 4'6-diamidino-2-phenylindole (DAPI). The immunostained slides were analyzed using a laser confocal microscope (LSM710, Carl Zeiss, Oberkochen, Germany). For quantitative analysis, we used Zeiss ZEN digital imaging software (RRID:SCR_013672) accompanied by the LSM 710 microscopy set by same detector gain, amplifier offset, and amplifier gain under a constant laser power in every set of the experiments. The intensity was calculated in randomly selected five 300×300 μm^2 areas from each section using 10 sections from one group which contains at least 3 rats. The quantification of the relative intensity was carried out by counting the relative number of the pixels showing each intensity unit.

Polymerase Chain Reaction

To quantify mRNA levels, total mRNA was prepared using the acid guanidine thiocyanate-phenol-chloroform extract method (Park et al., 2015). Three micrograms of mRNA were used for cDNA synthesis using SuperScriptII (Invitrogen, Calsbad, CA, USA). Then, cDNA served as the template for polymerase chain reaction (PCR) amplification using following primers: HO1-F, 5′-AGCATGTCCCAGGATTTGTC-3′; HO1-R, 5′-ACCAGCAGCTCAGGATGAGT-3′; HO2-F, 5′-GCA ATTCAAGCAGTTCTACC-3′; HO2-R, 5′-TGTAGTA CCAGGCCAAGAGT-3′; Glyceraldehyde-3-phosphate dehydrogenase (GAPDH)-F, 5′-CTACATG GTCTACATGTTCCAGTATG-3′; GAPDH-R, 5′-AG TTGTCATGGATGACCTTGG-3′. Real-time PCR reactions were conducted by 1 μL of cDNA as template, 5 μL of SYBR Green PCR master mix (Applied Biosystems, Warrington, UK), and 10 pmol of each primers. PCR amplifications were conducted using TP700 (Takara Bio Inc, Kusatsu, Japan). Next, to visualize mRNA levels, semiquantitative PCR reactions was conducted in 25 to 33 cycles for GAPDH, HO1, and HO2, and then, gel electrophoresis was performed to confirm the correct size of the amplified cDNA and the absence of nonspecific bands.

Western Blot Analysis

The extracted *in vivo* sciatic nerves were resuspended in a modified radioimmunoprecipitation assay buffer—50 mM Tris-HCl (pH 7.4), 150 mM NaCl, 0.5% deoxycholic acid, 0.5% Triton X-100, 1 mM phenylmethylsulfonyl fluoride, 1 mM sodium *o*–vanadate, 1× protease inhibitor cocktail tablet (Roche Molecular Biochemicals, Nutley, NJ, USA)]—boiled for 5 min and centrifuged for 10 min at 15,000 g at 4°C. The supernatants were resolved on 10% SDS-polyacrylamide gel and electroblotted onto nitrocellulose membrane (Millipore, Bedford, MA, USA). Blots were then blocked with 5% nonfat milk in Tris-buffered saline containing 0.05% Tween 20 and incubated with the appropriate antibodies (HRPs, RRID:AB_330924, 2099233). Blots were developed an enhanced chemiluminescence system (GE Healthcare, Chicago, IL, USA) and band intensity was quantified from X-ray films using the scanner and analyzed with the luminescence image analysis system (RRID:SCR_014299; Fujifilm, Tokyo, Japan).

Statistical Analysis

Data were collected randomly and tested in a blinded manner. All statistical analyses were conducted on at

least four independent experiments. All of the analyses (one-way ANOVA multiple comparison test) were performed using SPSS 21.0 software (RRID:SCR_002865; IBM, Armonk, NY, USA). Statistical details are reported in each result and figure legend.

Results

HO1 Is Highly Expressed in Injured Peripheral Nerve In Vivo

After peripheral nerve injury, oxidative events become the main causes of peripheral nerve degeneration (Valek et al., 2015; Lv et al., 2018). Thus, HOs, major proteins that arise as a result of oxidative events, likely have important roles during nerve degeneration and regeneration in the PNS. To determine which HOs affect peripheral nerve degeneration and regeneration, we first examined HO1 and HO2 mRNA expression levels by quantitative reverse transcription PCR *in vivo* using a sciatic nerve crush model. At 3 days after nerve injury, HO1 mRNA was highly expressed in sciatic nerve and its expression decreased during nerve regeneration (Figure 1(a)). In contrast, HO2 mRNA did not show altered expression (Figure 1(a)). To visualize the mRNA expression patterns of HO1 and HO2 in the sciatic nerve, we performed semiquantitative PCR using HO1, HO2, and GAPDH primers. Semiquantitative PCR revealed an increase in HO1 mRNA during nerve degeneration and a decrease during nerve regeneration (Figure 1(b)). Quantitative analysis (Figure 1(b)) revealed a peak increase in the HO1 mRNA level at 3 days after nerve injury, although no alteration in the HO2 mRNA level was observed during either whole-nerve degeneration or regeneration (Figure 1(c)).

Next, we identified the protein expression patterns of HO1 and HO2 *in vivo* using a sciatic nerve crush model. Similar to the mRNA expression patterns of HO1 and HO2, Western blot analysis showed that HO1 was highly expressed at 3 days after nerve injury and decreased during nerve regeneration (Figure 2(a) and (b)). After completion of nerve regeneration, HO1 protein level returned to the level of the control (Figure 2(a) and (b)). In addition, immunolabeling for HO1 with *in vivo*-teased sciatic nerve fiber samples showed that HO1 was highly expressed during nerve degeneration and the expression ceased during nerve regeneration, similar to the control (Figure 2(c) and (d)). Conversely, HO2 was continuously expressed in the sciatic nerve regardless of the condition. At 3 days after nerve injury, HO1 was expressed around the ovoid-like structures, not in their core (Figure 2(c)). Taken together, our results imply that, after nerve crush, HO1, not HO2, is the main enzyme that oxidizes cellular heme in the peripheral nerve and
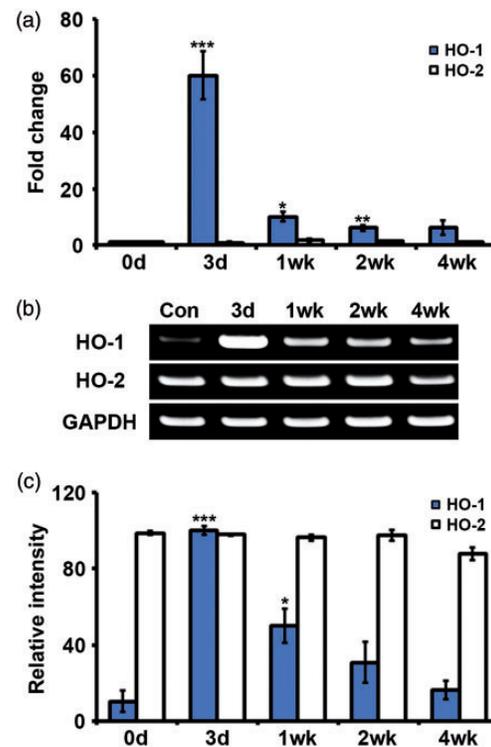
Figure 1. Expression patterns of HO mRNA during peripheral nerve degeneration and regeneration. (a) HO1 and HO2 mRNA levels were estimated by quantitative PCR using *in vivo* sciatic nerves during 1 month after nerve crush ($n = 6$). *$P < 0.01$, **$P < 0.001$, ***$P < 0.0001$. (b) HO1 and HO2 mRNA levels were visually confirmed by semiquantitative PCR using *in vivo* sciatic nerves during 1 month after nerve crush. (c) Quantitative analyses show relative intensities of HO1 and HO2 mRNA expressions of (b). *$P < 0.01$, ***$P < 0.0001$. HO = heme oxygenase; GAPDH = glyceraldehyde-3-phosphate dehydrogenase; loading control; Con = control (uninjured sciatic nerve).

is likely involved in oxidative events during Wallerian degeneration.

HO1 Is Highly Expressed in Denervated Schwann Cells In Vitro and In Vivo

Studies have used Western blot analysis of a cancer cell line and *in vivo* immunolabeling to show that HO1 is expressed in Schwann cells, albeit without comparison to other structures in peripheral nervous tissue (Hirata et al., 2000; Yama et al., 2016). To identify the exact location of HO1 activation in peripheral nervous tissue during Wallerian degeneration, we performed immunolabeling with S100 (a marker of Schwann cells) and (a marker of axons) antibodies. In the sciatic nerve cross-sections, HO1 immunostaining was highly increased at 3 days after nerve injury and highly overlapped with S100, but not NF, immunostaining (Figure 3 (a)). S100/HO1 or NF/HO1 double-positive cell counts
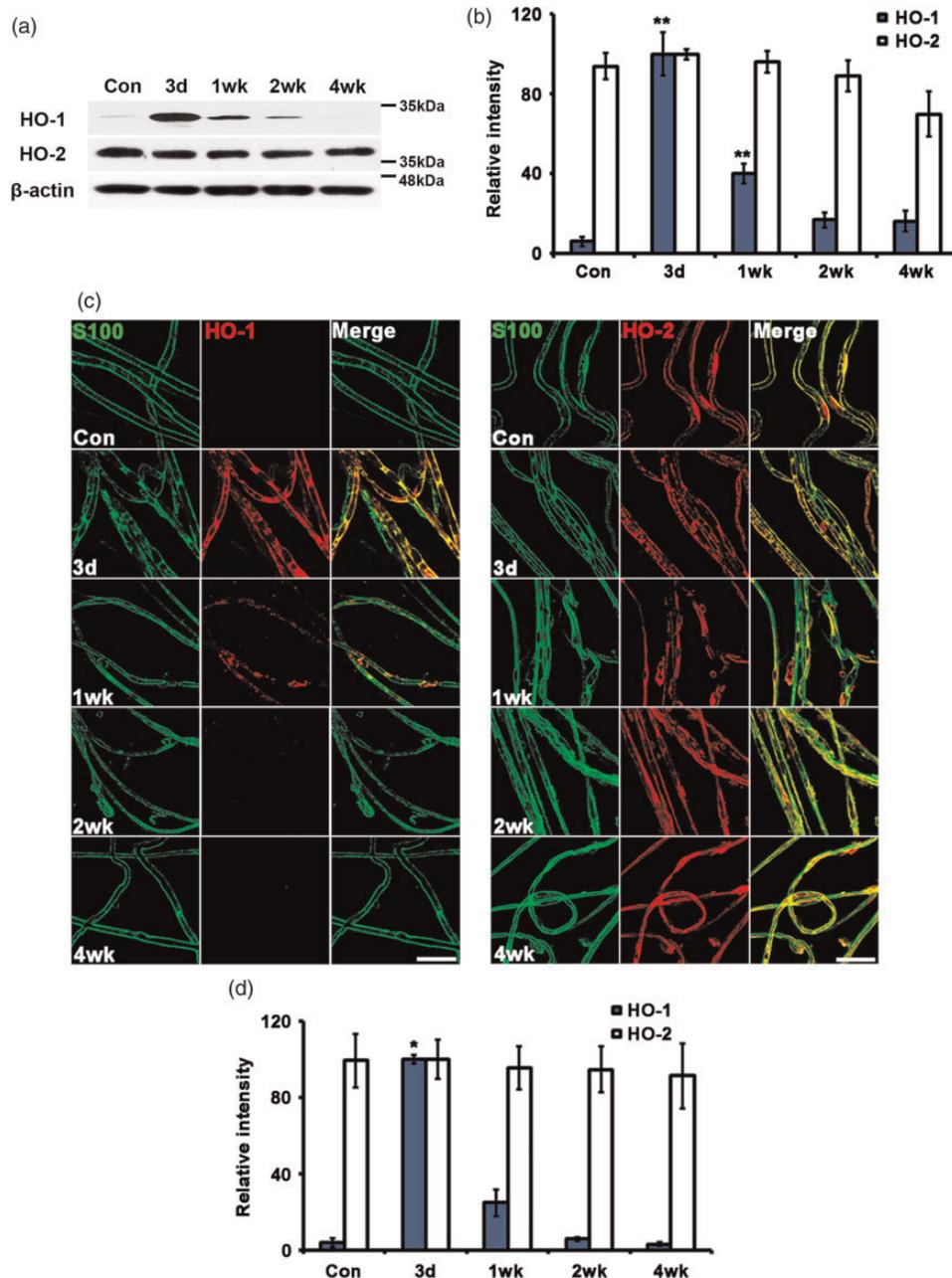
Figure 2. Expression patterns of HO protein during peripheral nerve degeneration and regeneration. (a) HO1 and HO2 protein levels were estimated by Western blot analysis using *in vivo* sciatic nerves during 1 month after nerve crush ($n = 6$). (b) Quantitative analyses show relative intensities of HO1 and HO2 protein expression of (a). **$P < 0.001$. (c) HO1 and HO2 protein levels were estimated by immunostaining with anti-S100 (green) as a marker of Schwann cells, anti-HO1 (red) and anti-HO2 (red) using *in vivo*-teased sciatic nerve fibers after nerve crush ($n = 4$ rats). Size bar = 50 μm. (d) Quantitative analyses show relative intensities of HO1 and HO2 protein expression with confocal images of (c). *$P < 0.01$. HO = heme oxygenase; Con = control (uninjured sciatic nerve).

also showed that HO1 activation occurred in the S100 immunostained area (Figure 3(b)). Although HO1 was not expressed in the whole Schwann cell, it was partially expressed around ovoid-like myelin fragments, a phenomenon of myelin breakage during Wallerian degeneration (arrowhead, Figure 3(c)). These results indicate that HO1 is highly expressed in denervated Schwann cells, not peripheral axons, and is located in the cytoplasm of Schwann cells excluding the degrading myelin sheath.

In mammalian cells, HO1 cleaves the heme ring to form biliverdin, CO, and ferrous iron. Thus, if HO1 is highly expressed in denervated Schwann cells, CO, a product of HO1, should also be highly expressed in
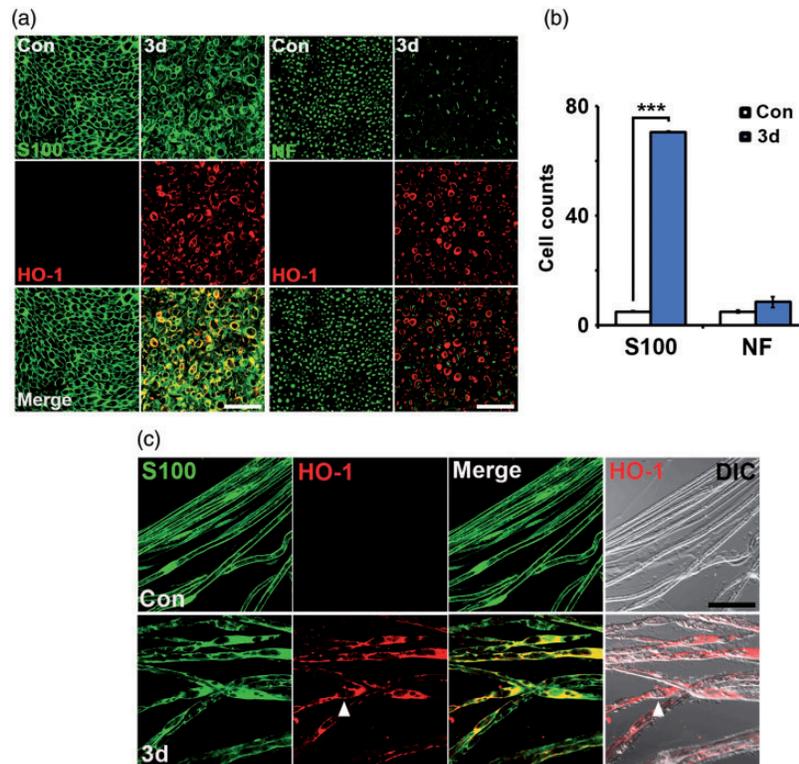
Figure 3. Denervated Schwann cells highly express HO1 during Wallerian degeneration. (a) Cross sections of *in vivo* sciatic nerves at 3 days after axotomy were immunostained with HO1 (red) and NF or S100 (green). Size bar = 50 μm. (b) Cell counts of (a) show the numbers of HO1/S100 or HO1/NF double-positive cells under a microscopic field (300 × 300 μm). ***$P < 0.0001$. $n = 4$ rats. (c) Immunostaining of *in vivo*-teased sciatic nerve fibers at 3 days after axotomy confirmed the overlapping between HO1 (red) and S100 (green) around ovoid-like structure. Size bar = 50 μm. HO = heme oxygenase; Con= control; NF = neurofilament; DIC= differential interference contrast.

denervated Schwann cells. To examine CO expression in denervated Schwann cells, we performed gaseous CO staining in a primary Schwann cell culture instead of *in vivo* Schwann cells, because in culture, Schwann cells are separated from axons and become denervated or enter into a dedifferentiated state. For CO staining in Schwann cells, we used a palladium-mediated fluorescent probe for CO-specific selection in living cells (Michel et al., 2012). In the primary Schwann cell culture, CO staining increased in a dose-dependent manner and was located in the cytoplasm, not the nucleus (Figure 4(a) and (b)). These results indicate that CO is highly expressed in denervated Schwann cells. Thus, CO, one of by-products of HO1 activation, is likely important in Schwann cell dynamics during Wallerian degeneration.

Regulation of HO1 Activation Ex Vivo Affects Myelin Fragmentation Process in the Peripheral Nerve

To identify the oxidative stress-mediated function of HO1 in Schwann cells during Wallerian degeneration, we screened several drugs that inhibit HO1 activation to abolish the function of HO1 in denervated Schwann

cells. For the screening, we used an *ex vivo* sciatic nerve explant culture system as described previously (Park et al., 2015). Based on the notion that the transverse stripe of the sciatic nerve disappears during Wallerian degeneration, we screened six drugs that inhibit HO1 activation: calmidazolium chloride (1 mM), lysophosphatidic acid (1 mM), zinc protoporphyrin (2, 20, and 200 μM), chromium mesoporphyrin (CrMP, 50 and 500 μM), tin mesoporphyrin (SnMP, 10 μM and 1 mM), and tin protoporphyrin (SnPP, 10 and 100 μM) (Vreman et al., 1993; Wagner et al., 2000; Koeppen and Dickson, 2002; Boehning et al., 2004; Nowis et al., 2008; Xie et al., 2014). Of the HO1-inhibitory drugs, CrMP (50 μM), SnMP (1 mM), and SnPP (10 μM) strongly inhibited the disappearance of transverse stripes at 3 days *in vitro* (3DIV) during Wallerian degeneration *ex vivo* (Figure 5(a)). Quantitative analysis also showed the inhibitory effects of CrMP (50 μM), SnMP (1 mM), and SnPP (10 μM) on Wallerian degeneration (Figure 5 (b)). In addition, we investigated whether three drugs suppress oxidative stress during Wallerian degeneration using nitric oxide synthases (NOS1 and NOS2) as markers of nitrogen-free radical species. Western blot
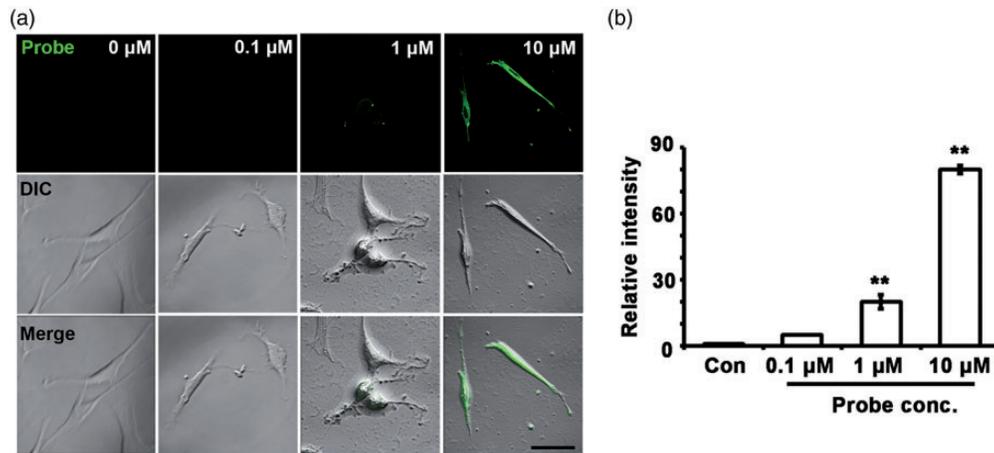
Figure 4. Carbon monoxide (CO) is highly expressed in primary Schwann cells. (a) CO-specific fluorescent probe (green) staining shows dose-dependent CO expression in primary Schwann cell culture. Size bar $= 20\ \mu$m. (b) Quantitative analysis of (a) shows relative intensity of CO-specific fluorescent probe staining ($n = 3$ rats). **$P < 0.001$. DIC $=$ differential interference contrast; Con $= 0\ \mu$M probe.
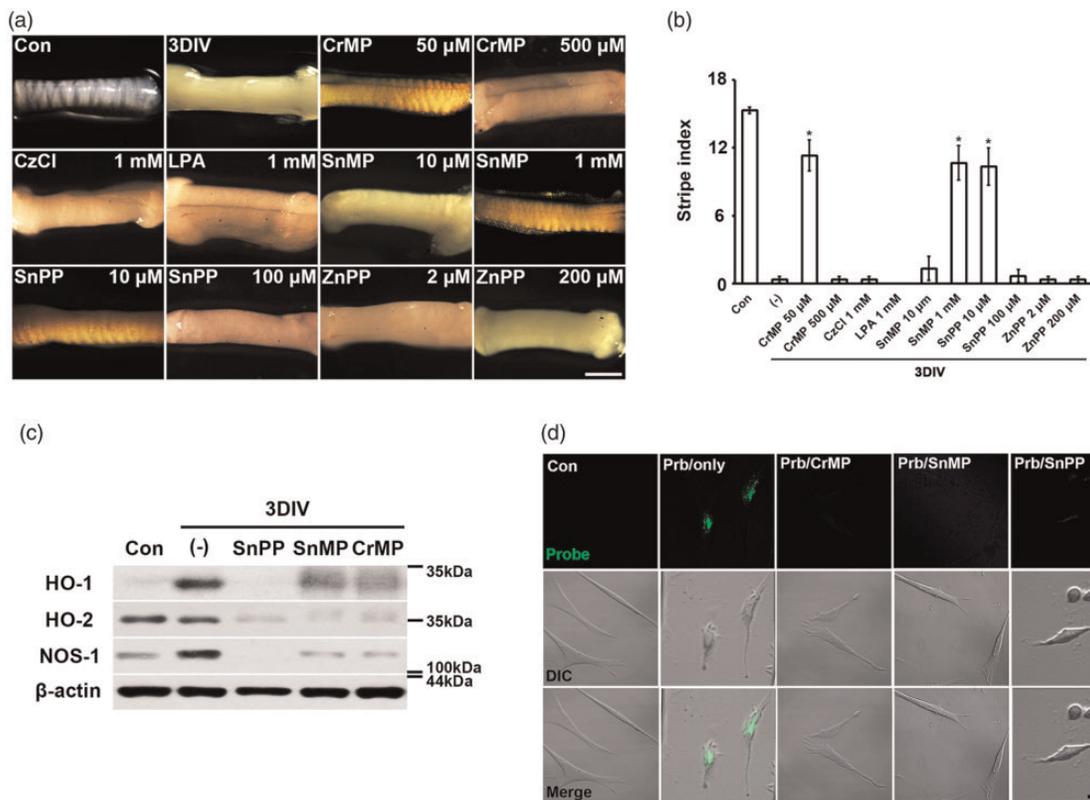
Figure 5. Inhibition of HO1 activation protects against demyelination. (a) Sciatic nerve explants were cultured for 3DIV with or without HO1 inhibitors and then the explants were visualized under a stereoscope. Size bar $= 600\ \mu$m. (b) Quantitative graph of (a) shows the number of transverse stripe within 2 mm of a sciatic nerve explant under a stereoscope (stripe index). $n = 4$ rats. *$P < 0.01$. (c) Western blot analysis shows the expression levels of HO1, HO2, and neuronal NOS1 as a marker for oxidative stress ($n = 4$ rats). (d) CO-specific probe staining show the inhibitory effect of CrMP, SnMP, and SnPP on production of CO in primary Schwann cell culture. Scale size $= 20\ \mu$m. 3DIV $= 3$ days *in vitro*; CrMP $=$ chromium mesoporphyrin; CzCl $=$ calmidazolium chloride; LPA $=$ lysophosphatidic acid; SnMP $=$ tin mesoporphyrin; SnPP $=$ tin protoporphyrin; ZnPP $=$ zinc protoporphyrin; HO $=$ heme oxygenase; NOS $=$ nitric oxide synthase; DIC $=$ differential interference contrast; Con $=$ control (uninjured sciatic nerve); Prb $=$ probe.

analysis showed that NOS1 was highly expressed on 3DIV (Figure 5(c)). By contrast, CrMP, SnMP, and SnPP treatments inhibited the increases in NOS1 on 3DIV, with levels similar to the control (Figure 5(c)). These inhibitory effects of three drugs mean that HOs activation regulates oxidative stress during Wallerian degeneration. Interestingly, NOS2 protein expression was not found in the Western blot analysis (data not shown) because NOS2 is not present in sciatic nerves (Kikuchi et al., 2018). These three drugs also inhibited HO2 on 3DIV because CrMP, SnMP, and SnPP by competing with heme for binding HOs suppress both HO1 and HO2 (Figure 5(c)). These three drugs effectively suppressed CO expression via HO1 activation in the primary Schwann cell culture (Figure 5(d)). These three inhibitory drugs (CrMP, SnMP, and SnPP) also effectively inhibited HO1 activation up to CO expression against oxidative stress. Thus, our results imply that HO1 activation regulates Wallerian degeneration in Schwann cells against oxidative stress. To assess the detailed subfunctions of HO1 in Schwann cells further, we used three drugs: CrMP (50 μM), SnMP (1 mM), and SnPP (10 μM).

Next, to identify whether HO1 affects myelin fragmentation process, a phenomenon of Wallerian degeneration, we performed morphometric approaches using DIC microscopic analysis of Schwann cells and immunolabeling with MBP (a marker of the myelin sheath) antibody in *ex vivo*-teased sciatic fibers. Because myelin fragmentation process takes on an ovoid-like shape which appears on the surface of sciatic nerve fibers (Jung et al. 2011a; Park et al. 2015). DIC microscopic analysis revealed that the inhibition of HO1 activation in *ex vivo* sciatic nerve suppressed the appearance of ovoid-like myelin fragments at 3DIV, similar to the control (arrows) (Figure 6(a)). Morphometric analysis of ovoid formation showed that CrMP, SnMP, and SnPP effectively reduced the number of ovoids at 3DIV in the teased nerve fibers (Figure 6(b)). In addition, confocal microscopy revealed consecutive MBP-immunostained double lines in both margins of control sciatic nerve (Figure 6(c)). In contrast, at 3DIV, the continuity of MBP immunostaining was broken down and was located mainly in the ovoid core; however, inhibition of HO1 maintained intact lines, similar to the control (Figure 6 (c)). Quantitative analysis also revealed significant suppression of the breakage of myelin sheath double lines (Figure 6(d)). Thus, these results indicate that oxidative stress-mediated HO1 activation affects myelin fragmentation process during Wallerian degeneration.

Regulation of HO1 Activation Ex Vivo Affects Schwann Cell Transdedifferentiation in the Peripheral Nerve

During Wallerian degeneration, Schwann cells are recharacterized to be similar, but not identical, to developmental Schwann cells. These specific Schwann cells that arise during Wallerian degeneration are known as transdedifferentiated or repair Schwann cells (Jessen and Mirsky, 2016). To determine whether HO1 activation is related to Schwann cell transdedifferentiation, we performed immunolabeling with Schwann cell transdedifferentiation markers, LAMP1 and p75 antibodies (Jung et al., 2011b). Confocal microscopy showed that at 3DIV, the intensities of LAMP1 and p75 immunostaining were highly increased compared with the control. In contrast, inhibition of HO1 activation suppressed LAMP1 and p75 expression at 3DIV (Figure 7(a)). Quantitative analysis revealed that CrMP, SnMP, and SnPP effectively inhibited the expression of LAMP1 and p75 in the *ex vivo* sciatic nerve fibers (Figure 7(b)). Thus, these results suggest that HO1 leads to Schwann cell transdedifferentiation during Wallerian degeneration *ex vivo*.

Regulation of HO1 Activation Ex Vivo Affects Schwann Cell Proliferation in the Peripheral Nerve

The proliferation of Schwann cells is another feature of note in Wallerian degeneration. To determine whether HO1 activation affects Schwann cell proliferation during Wallerian degeneration, we performed immunolabeling with a cell proliferation marker, Ki67 antibody. Confocal microscopy showed that at 3DIV, Ki67 immunostaining highly overlapped with DAPI staining (Figure 8(a)). In contrast, HO1-inhibitory drugs suppressed the induction of Ki67 in Schwann cells (Figure 8(a)). Quantitative cell counts also showed that at 3DIV, inhibition of HO1 activation abolished the induction of Ki67 in Schwann cells (Figure 8(b)). Thus, these results indicate that HO1 leads to Schwann cell proliferation during Wallerian degeneration *ex vivo*.

Regulation of HO1 Activation In Vivo Affects Myelination Fragmentation Process and Axonal Degradation During Wallerian Degeneration

To confirm the relevance of HO1 on Wallerian degeneration, we performed morphometric analyses using the stripe, ovoid, myelin, and NF indices in *in vivo* model. We used a 10-mm blind PVC tube packed with gel foam presoaked in CrMP (50 μM, 500 μM, and 5 mM), SnMP (100 μM, 1 mM, and 10 mM) and SnPP (10 μM, 100 μM, and 1 mM) to treat the distal stumps of axotomized sciatic nerves for 3 days (Park et al. 2015). In *in vivo* sciatic nerves treated with HO inhibitors for 3 days after axotomy, 5 mM CrMP, 10 mM SnMP, and 1 mM SnPP were most effective doses for inhibition of transverse stripes (Figure 9(a)). HO inhibitors also inhibited myelin fragmentation process during Wallerian degeneration *in vivo* after 3 days based on the number of ovoid fragments and
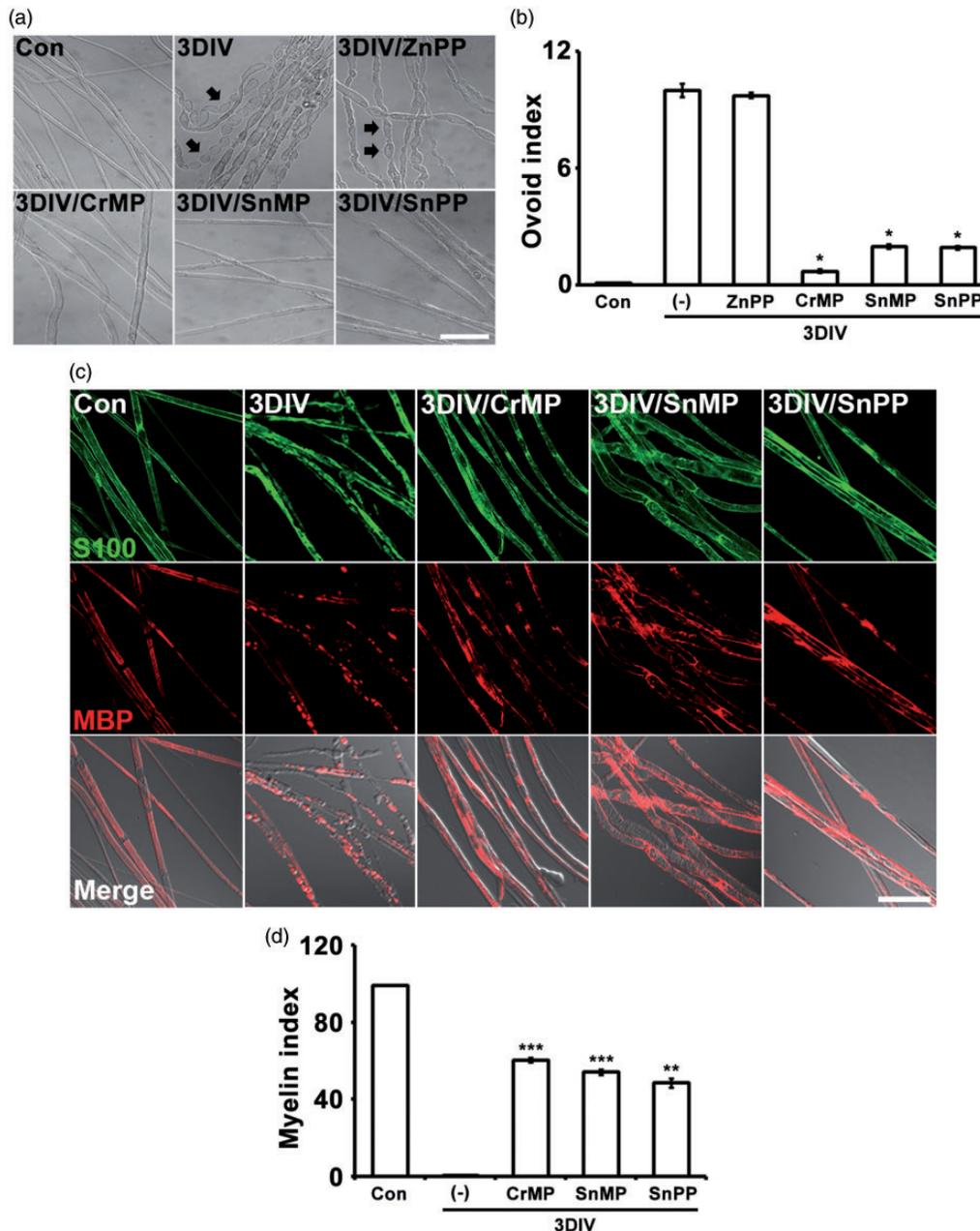
Figure 6. Inhibition of HO1 activation in Schwann cells preserves myelin sheaths in injured peripheral nerves. (a) Images of teased nerve fibers at 3DIV show ovoid-like myelin fragmentations. Size bar = 50 μm. (b) Quantitative graph of (a) shows the number of myelin ovoid (arrows) within 200 μm of a teased nerve fiber under a DIC-filtered microscope. ZnPP is a negative control. **$P < 0.001$. $n = 4$ rats. (c) Immunolabeling of MBP (a marker of myelin sheath, red) with S100 (green) antibody. Size bar = 50 μm. (d) Quantitative graph of (c) (myelin index) shows the number of nerve fibers which have intact double-lined immunostatining with longer than 50 μm among 100 teased nerve fibers under a microscopic field ($n = 4$ rats). **$P < 0.001$ and ***$P < 0.0001$. CrMP = chromium mesoporphyrin; SnMP = tin mesoporphyrin; SnPP = tin protoporphyrin; ZnPP = zinc protoporphyrin; DIC = differential interference contrast; MBP = myelin basic protein; Con = control (uninjured sciatic nerve); 3DIV = 3 days *in vitro*.

MBP immunostaining (Figure 9(b) to (d)). Next, we analyzed quantitatively the degree of axon preservation *in vivo* during Wallerian degeneration, using NF immunostaining after treatment of HO inhibitors (Figure 9(e)). Three HO inhibitors also suppressed the disappearance of consecutive NF-positive line structures in sciatic nerve fibers on 3DIV. Thus, we found that *in vivo* treatment with HO inhibitors effectively inhibited myelin fragmentation process and axonal degradation, suggesting that HO1 regulates Wallerian degeneration *in vivo*.
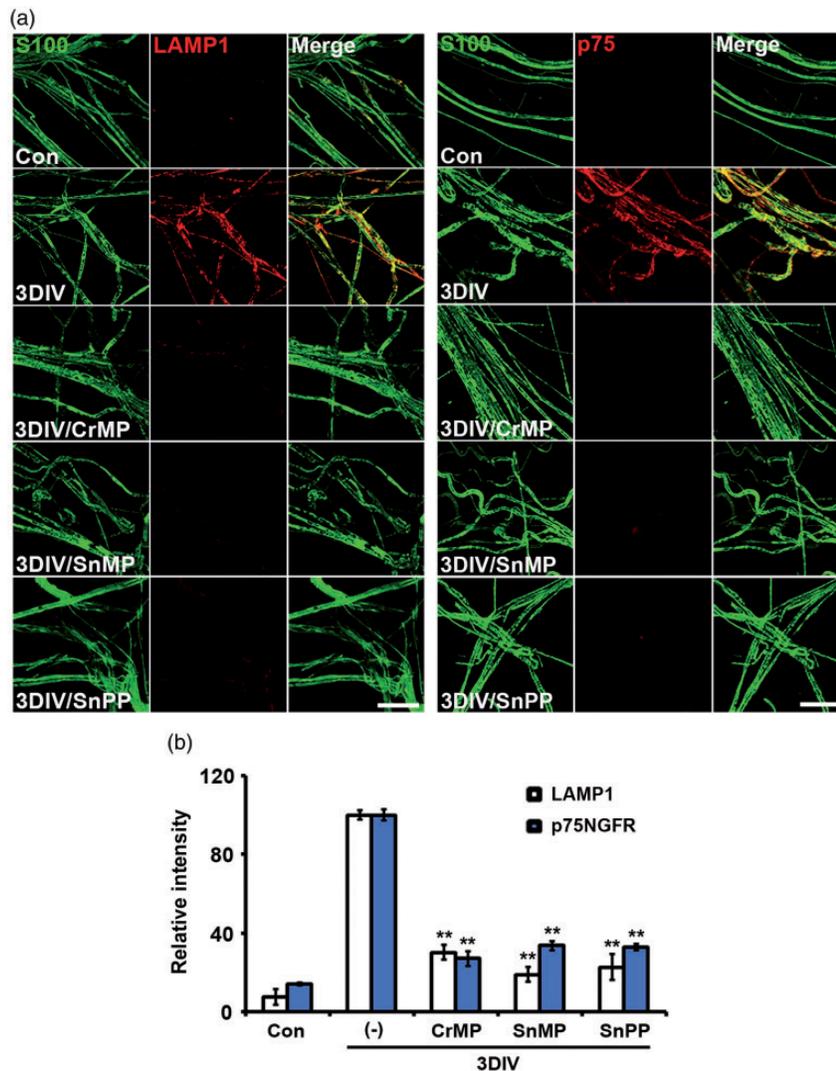
Figure 7. Inhibition of HO1 activation in Schwann cells regulates Schwann cell transdedifferentiation *ex vivo*. (a) Confocal images show immunolabeling for S100 (green) with LAMP1 (red) and p75 neurotrophin receptor (p75, red) as markers of Schwann cell transdedifferentiation using teased sciatic nerve fibers. Size bar = 100 μm. (b) Quantitative graph of (a) shows the relative intensities of LAMP1 and p75 (n = 4 rats). **$P < 0.001$. CrMP = chromium mesoporphyrin; SnMP = tin mesoporphyrin; SnPP = tin protoporphyrin; Con = control (uninjured sciatic nerve); 3DIV = 3 days *in vitro*.

Discussion

Expression Patterns of HOs in the Peripheral Nerve

HOs are mediators of oxidative injury and cellular stress in living cells and affect cellular redox homeostasis. Compared to the central nervous system, the roles of HOs in the PNS remain unknown. Hirata et al. (2000) reported high HO1 activation in myelin-phagocytosing Schwann cells in *in vivo*-injured sciatic nerves, and Yama et al. (2016) reported that upregulation of HO1 *in vitro* exerted neuroprotective effects. However, these studies did not determine which type of HOs was important in the PNS and which cell type (e.g., peripheral axons or Schwann cells) expressed HOs under specific conditions.

In addition, the authors did not describe the detailed functions of HOs during Wallerian degeneration.

When we first examined the distribution of HO1 and HO2 activation in peripheral nerves, we found that HO2 was always expressed in peripheral nerves with or without nerve injury (Figures 1 and 2). This finding indicates that in the PNS, HO2 likely acts to maintain normal levels of CO and ferrous iron as a way of surviving in living cells. In contrast, the activation of HO1 differed from that of HO2 in peripheral nerves. HO1 was highly expressed in denervated Schwann cells during Wallerian degeneration and decreased in reinnervated Schwann cells during nerve regeneration (Figures 1 and 2). These results are similar to those reported by Hirata et al.
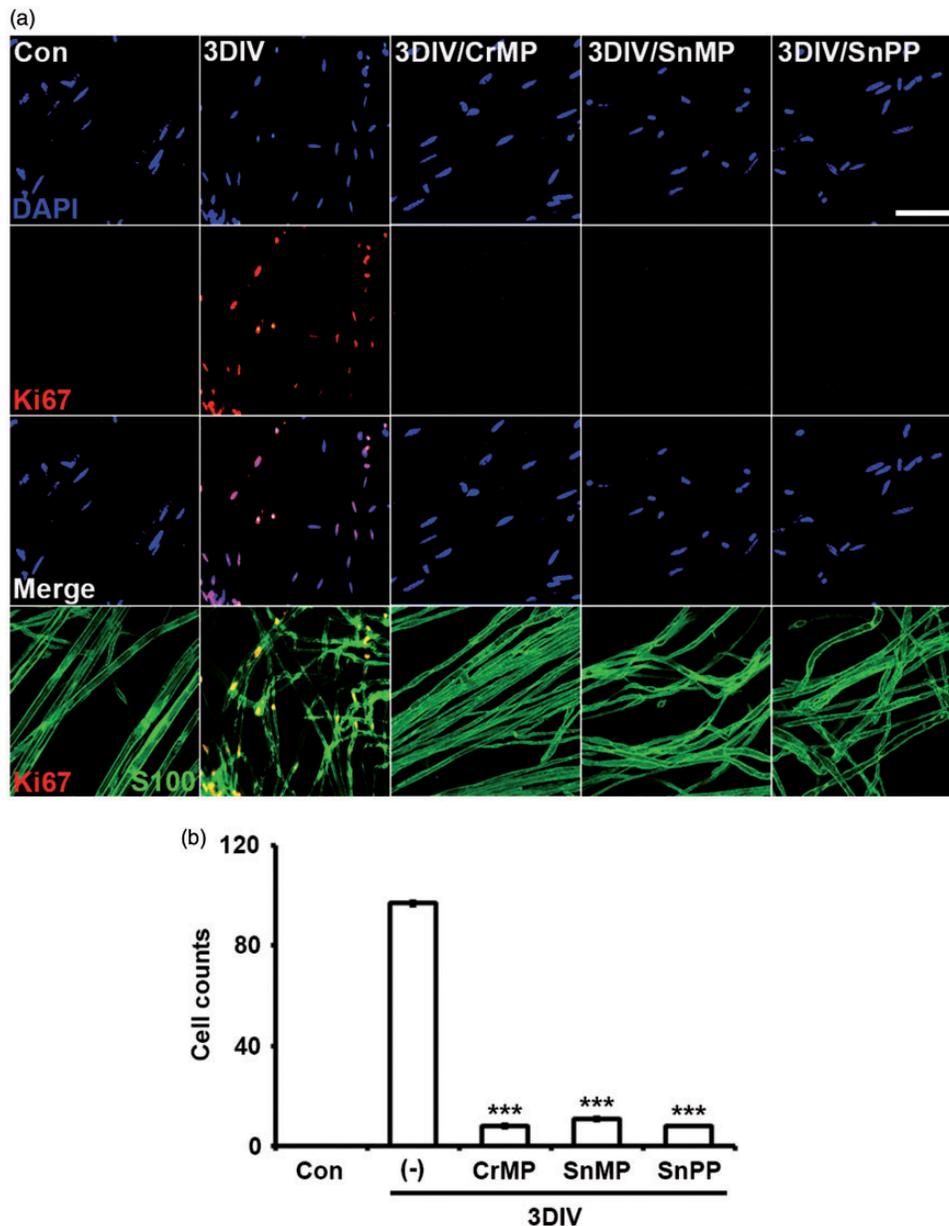
Figure 8. Inhibition of HO1 activation in Schwann cells regulates Schwann cell proliferation *ex vivo*. (a) Confocal images show staining for DAPI (blue) with S100 (green) and Ki67 (red) as a marker of cell proliferation. Size bar = 50 μm. (b) Quantitative graph of (a) shows the number of cells with Ki67 immunolabeling out of 200 DAPI-positive nuclei as compared with that of the control ($n = 4$ rats). ***$P < 0.0001$. CrMP = chromium mesoporphyrin; SnMP = tin mesoporphyrin; SnPP = tin protoporphyrin; Con = control (uninjured sciatic nerve); 3DIV = 3 days *in vitro*.

(2000), but are not consistent with those of Yama et al. (2016). According to Yama et al. (2016), epalrestat induced HO1 activation in Schwann-cell-related cells but did not promote induction of ferrous iron and reactive oxygen species. These results imply that epalrestat may exert an inhibitory effect on ferrous iron and reactive oxygen species, but not a direct effect on HO1. The increase in HO1 activation in Schwann-cell-related cells via epalrestat may compensate for the lack of ferrous iron in living cells. Thus, in peripheral nerves, HO1 may be upregulated when the nerve is damaged by oxidative injury.

On the other hands, because oxidative stress affects peripheral axon degeneration (Bros et al., 2014), we hypothesized that HO1 would be expressed in both injured Schwann cells and peripheral axons. However, HO1 was expressed only in Schwann cells, not in degenerating axons (Figure 3). These results indicate that in the peripheral nerve, the response to oxidative damage differs between Schwann cells and axons.
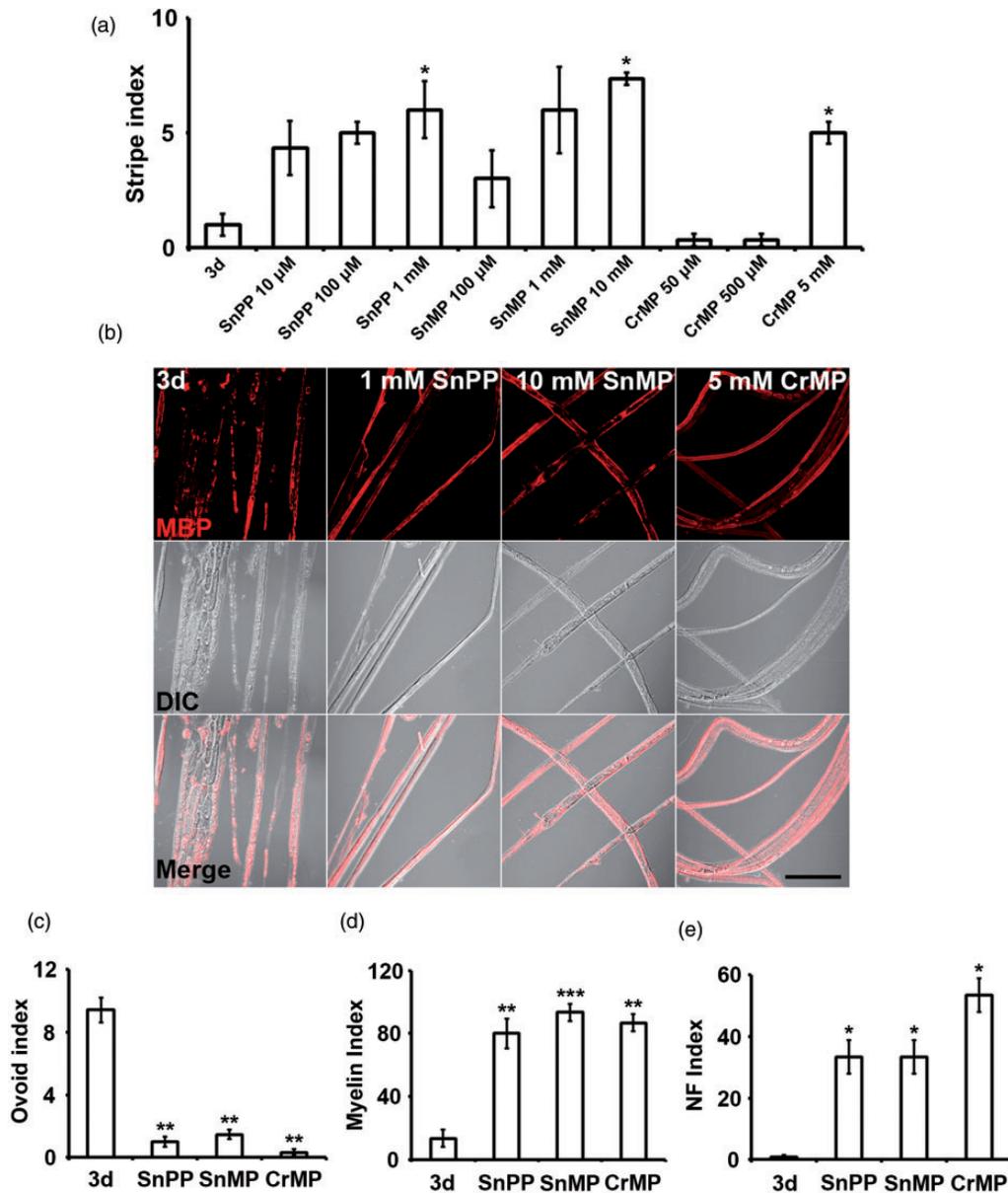
Figure 9. Inhibition of HO1 activation in *in vivo* animal model after nerve axotomy suppresses phenotypes of Wallerian degeneration in sciatic nerves. (a) The number of stripes (stripe index) are counted on sciatic nerve explants with the dose-dependent *in vivo* treatments of CrMP, SnMP and SnPP (*n* = 3 rats). In *in vivo* sciatic nerves, 5 mM CrMP, 10 mM SnMP and 1 mM SnPP were effective to inhibition of nerve degeneration. *$P < 0.05$. (b) Teased sciatic nerve fibers are immunostained for MBP (red). Ovoid structures are analyzed in teased nerve fibers under a DIC-filtered microscope. Size bar = 50 μm. (c,d,e) Quantification shows ovoid index and myelin index, respectively (*n* = 3 rats). **$P < 0.01$ and ***$P < 0.001$. (f) Morphometric analysis of axonal degradation is performed by NF index (*n* = 3 rats). *$P < 0.05$. CrMP = chromium mesoporphyrin; SnMP = tin mesoporphyrin; SnPP = tin protoporphyrin; DIC = differential interference contrast; MBP = myelin basic protein; NF = neurofilament.

Prooxidant Functions of HO1 in Schwann Cells During Wallerian Degeneration

In Schwann cells, after nerve injury, HO1 activation was highly upregulated 3 days (peak increase) during Wallerian degeneration, decreased during nerve regeneration, and ultimately disappeared, similar to the control. HO1 degrades heme into equimolar amounts of biliverdin, CO, and ferrous iron. Based on these products, HO1 exerts two contradictory antioxidant and prooxidant functions. Biliverdin and CO act as antioxidants and mediate cytoprotective effects (Ryter et al., 2006). In brain neurodegenerative diseases, HO1 plays a neuroprotective role against oxidative stress (Chen et al., 2000; Chen, 2014). In contrast, HO1 induction is associated with adverse effects in several diseases

(Schipper et al., 2009). For example, chronic activation of HO1 leads to pathological iron deposition in several neurodegenerative diseases, including Alzheimer's and Parkinson's, and induces irreversible neurological brain damage (Schipper and Song, 2015)

In peripheral nerves, the molecular mechanism of neurodegeneration associated with HO1-mediated oxidative events remains unclear. Our data imply that inhibition of HO1 suppresses peripheral nerve degeneration (Figures 5, 6 and 9) and important phenotypes of Wallerian degeneration, such as Schwann cell transdedifferentiation and proliferation (Figures 7 and 8). This functional inhibition of HO1 activation helps to explain the role of HO1 in specially denervated Schwann cells during Wallerian degeneration: Its prooxidant effect, rather than its antioxidant effect, tends to induce peripheral nerve degeneration (prooxidant effect > antioxidant effect). It was previously reported that transferrin, an iron carrier protein, is upregulated in Schwann cells after nerve injury (Hirata et al., 2000; Salis et al., 2007). These results support our hypothesis that after nerve injury, the prooxidant effect by iron deposition in Schwann cells is the main function of HO1 overexpression in Wallerian degeneration.

Effects of HO1 on Demyelination During Wallerian Degeneration

During Wallerian degeneration, peripheral nerves morphologically show two appearances: (i) axon degradation and (ii) demyelination. Axons can be broken down either directly via neuronal cellular mechanisms (Fischer et al., 2012; Bros et al., 2014) or indirectly by mechanical force from Schwann cells (Jung et al., 2011a). However, it appears that oxidative stress-mediated HO1 activation is not related to axonal degradation during Wallerian degeneration because HO1 is not expressed in peripheral axons (Figure 3). This result indicates that HO1 in Schwann cell dynamics is more important than peripheral axons during Wallerian degeneration. Previous studies have shown that Schwann cell demyelination is regulated by the MAPK pathway (Parkinson et al., 2008; Yang et al., 2012), and our results indicate that HO1 inhibition in Schwann cells suppresses myelin fragmentation process (Figures 5 and 6). These results indicate that the inhibition of demyelination by HO1 inhibitory drug treatment in sciatic nerve explant cultures may be because CO, a product of HO1, acts as a cell signaling molecule which affects the increase in c-jun and p38 MAPK expression in Schwann cells (Lee and Chau, 2002; Morse et al., 2003). Interestingly, in Figures 5 and 6, each HO inhibitor showed different HO-inhibitory effect and inhibited incompletely ovoid formation. Almost HO inhibitors compete with heme to suppress HO activation in living cells (Vreman et al.,

1993; Wagner et al., 2000; Koeppen and Dickson, 2002; Boehning et al., 2004; Nowis et al., 2008; Xie et al., 2014). HO inhibitors contain a ring structure which binds to iron and competes with heme protein for binding to iron. However, because this structure is little bit bulky and each inhibitor contains a different positive metal ion in the core of a ring, they have different chemical characterics, such as permeability, solubility and stability. In addition, because sciatic nerves consist of three-layered connective membranes (epineurium, perineurium, and endoneurium), it is not easy for the inhibitors to penetrate into Schwann cells effectively. Thus, these may be main reasons why all inhibitors could show different drug effects on *ex vivo* sciatic nerve explants and inhibit incompletely the nerve degeneration. In addition, oxidative stress in Schwann cells can modify lipid profiles and induce myelin disruption during Wallerian degeneration (Hichor et al., 2017, 2018). Thus, the induction of demyelination during Wallerian degeneration may be because overproduction of ferrous iron, a by-product of HO1, deteriorates oxidative conditions in Schwann cells and induces demyelination or prompts demyelination in Schwann cells. To visualize clearly the effect of HO1 activation on demyelination, further evaluation, such as analysis of semithin or ultrathin sections, should be necessary.

Effects of HO1 on Schwann Cell Transdedifferentiation and Proliferation During Wallerian Degeneration

During Wallerian degeneration, Schwann cells undergo recharacterization to become similar, but not identical, to developmental Schwann cells. The state of the recharacterized Schwann cell is called transdedifferentiation, and such Schwann cells are known as dedifferentiated or repair Schwann cells (Jessen and Mirsky 2016). Thus, Schwann cell transdedifferentiation is a phenotype of Wallerian degeneration in the PNS. The suppression of Schwann cell transdedifferentiation by HO1 inhibition observed in this study demonstrates that HO1 activation regulates the expression of transdedifferentiation-related molecules at the intracellular level in Schwann cells (Figure 7). It was previously reported that oxidative stress induced p75NTR expression, leading to neurodegeneration (Shin et al., 2011; Kraemer et al., 2014), and lysosomal expression, leading to apoptotic cell death (Kurz et al., 2008; Yoon et al., 2011). Thus, p75NTR and lysosomal expression can be used as molecular markers for oxidative stress-mediated Schwann cell transdedifferentiation (Jung et al., 2011b). Our data also indicate that HO1 inhibition suppresses induction of both p75NTR and LAMP1 (a lysosomal protein) (Figure 7), implying that the decreased prooxidant effects of HO1 inhibition suppress induction of p75NTR and

lysosomal expression in Schwann cells during Wallerian degeneration.

Finally, HO1-expressing cells show uncontrolled proliferation and progress toward carcinogenesis and metastasis (Nitti et al., 2017). Denervated Schwann cells also share features with cancer cells, such as cell proliferation and epithelial–mesenchymal transition. In our study, during Wallerian degeneration, Schwann cells underwent proliferation, while HO1 inhibition suppressed Schwann cell proliferation (Figure 8). These results imply that oxidative events induced by HO1 activation in denervated Schwann cells influence Schwann cell proliferation during Wallerian degeneration.

In conclusion, our results demonstrated pathophysiological roles of HO1 that regulate myelin fragmentation process, axonal degradation, Schwann cell transdedifferentiation, and proliferation during Wallerian degeneration. In addition, we identified that HO regulates for the first time CO expression in Schwann cells using synthetic CO-specific probe morphologically. Thus, we define HO1/CO as new regulators in Schwann cells during Wallerian degeneration.

Author Contributions

M. K., H. K., D. G. K., D. K. K., H. J. C., J. J., and N. Y. J. designed this study and interpreted experimental results. J. J. and N. Y. J. defined intellectual contents. M. K., H. K., D. G. K., H. J. C., J. J., Y. H., C. P., and N. Y. J. performed experiments and wrote the manuscript. All authors approved the final version of this paper.

Declaration of Conflicting Interests

The author(s) declared no potential conflicts of interest with respect to the research, authorship, and/or publication of this article.

ORCID iD

Junyang Jung ⓘ http://orcid.org/0000-0003-3946-5406

References

Boehning, D., Sedaghat, L., Sedlak, T. W., & Snyder, S. H. (2004). Heme oxygenase-2 is activated by calcium-calmodulin. *J Biol Chem*, 23, 30927–30930.

Bros, H., Millward, J. M., Paul, F., Niesner, R., & Infante-Duarte, C. (2014). Oxidative damage to mitochondria at the nodes of Ranvier precedes axon degeneration in ex vivo transected axons. *Exp Neurol*, 261, 127–135.

Caillaud, M., Chantemargue, B., Richard, L., Vignaud, L., Favreau, F., Faye, P. A., Vignoles, P., Sturtz, F., Trouillas, P., Vallat, J. M., Desmoulière, A., & Billet, F. (2018). Local low dose curcumin treatment improves functional recovery and remyelination in a rat model of sciatic nerve crush through inhibition of oxidative stress. *Neuropharmacology*, 139, 98–116

Chen, J. (2014). Heme oxygenase in neuroprotection: From mechanisms to therapeutic implications. *Rev Neurosci*, 25, 269–280.

Chen, K., Gunter, K., & Maines, M. D. (2000). Neurons over-expressing heme oxygenase-1 resist oxidative stress-mediated cell death. *J Neurochem*, 75, 304–313.

D'Aguanno, S., Franciotta, D., Lupisella, S., Barassi, A., Pieragostino, D., Lugaresi, A., Centonze, D., D'Eril, G. M., Bernardini, S., Federici, G., & Urbani, A. (2010). Protein profiling of Guillain-Barrè syndrome cerebrospinal fluid by two-dimensional electrophoresis and mass spectrometry. *Neurosci Lett*, 485, 49–54.

Dwyer, B. E., Nishimura, R. N., & Lu, S. Y. (1995). Differential localization of heme oxygenase and NADPH-diaphorase in spinal cord neurons. *Neuroreport*, 6, 973–976.

Fischer, L. R., Li, Y., Asress, S. A., Jones, D. P., & Glass, J. D. (2012). Absence of SOD1 leads to oxidative stress in peripheral nerve and causes a progressive distal motor axonopathy. *Exp Neurol*, 233, 163–171.

Hichor, M., Sampathkumar, N. K., Montanaro, J., Borderie, D., Petit, /1. /2, Gorgievski, V., Tzavara, E. T., Eid, A. A., Charbonnier, F., Grenier, J., & Massaad, C. (2017). Paraquat induces peripheral myelin disruption and locomotor defects: Crosstalk with LXR and Wnt pathways. *Antioxid Redox Signal*, 27, 168–183.

Hichor, M., Sundaram, V. K., Eid, S. A., Abdel-Rassoul, R., Petit, P. X., Borderie, D., Bastin, J., Eid, A. A., Manuel, M., Grenier, J., & Massaad, C. (2018). Liver X receptor exerts a protective effect against the oxidative stress in the peripheral nerve. *Sci Rep*, 8, 2524.

Hirata, K., He, J. W., Kuraoka, A., Omata, Y., Hirata, M., Islam, A. T., Noguchi, M., & Kawabuchi, M. (2000). Heme oxygenase1 (HSP-32) is induced in myelin-phagocytosing Schwann cells of injured sciatic nerves in the rat. *Eur J Neurosci*, 12, 4147–4152.

Jessen, K. R., & Mirsky, R. (2016). The repair Schwann cell and its function in regenerating nerves. *J Physiol*, 594, 3521–3531.

Jung, J., Cai, W., Lee, H. K., Pellegatta, M., Shin, Y. K., Jang, S. Y., Suh, D. J., Wrabetz, L., Feltri, M. L., & Park, H. T. (2011a). Actin polymerization is essential for myelin sheath

fragmentation during Wallerian degeneration. *J Neurosci*, *31*, 2009–2015.

Jung, J., Cai, W., Jang, S. Y., Shin, Y. K., Suh, D. J., Kim, J. K., & Park, H. T. (2011b). Transient lysosomal activation is essential for p75 nerve growth factor receptor expression in myelinated Schwann cells during Wallerian degeneration. *Anat Cell Biol*, *44*, 41–49.

Kikuchi, K., Ambe, K., Kon, H., Takada, S., & Watanabe, H. (2018). Nitric oxide synthase (NOS) Isoform expression after peripheral nerve transection in mice. *Bull Tokyo Dent Col*, *59*, 15–25.

Koeppen, A. H., & Dickson, A. C. (2002). Tin-protoporphyrin prevents experimental superficial siderosis in rabbits. *J Neuropathol Exp Neurol*, *61*, 689–701.

Kraemer, B. R., Snow, J. P., Vollbrecht, P., Pathak, A., Valentine, W. M., Deutch, A. Y., & Carter, B. D. (2014). Role for the p75 neurotrophin receptor in axonal degeneration and apoptosis induced by oxidative stress. *J Biol Chem*, *289*, 21205–21216.

Kurz, T., Terman, A., Gustafsson, B., & Brunk, U. T. (2008). Lysosomes and oxidative stress in aging and apoptosis. *Biochim Biophys Acta*, *1780*, 1291–1303.

Lee, T. S., & Chau, L. Y. (2002). Heme oxygenase-1 mediates the anti-inflammatory effect of interleukin-10 in mice. *Nat Med*, *8*, 240–246.

Lv, W., Deng, B., Duan, W., Li, Y., Liu, Y., Li, Z., Xia, W., & Li, C. (2018). Schwann cell plasticity is regulated by a weakened intrinsic antioxidant defense system in acute peripheral nerve injury. *Neuroscience*, *382*, 1–13.

Maines, M. D. (1997). The heme oxygenase system: A regulator of second messenger gases. *Annu Rev Pharmacol Toxicol*, *37*, 517–554.

Michel, B. W., Lippert, A. R., & Chang, C. J. (2012). A reaction-based fluorescent probe for selective imaging of carbon monoxide in living cells using a palladium-mediated carbonylation. *J Am Chem Soc*, *134*, 15668–15671.

Morse, D., Pischke, S. E., Zhou, Z., Davis, R. J., Flavell, R. A., Loop, T., Otterbein, S. L., Otterbein, L. E., & Choi, A. M. (2003). Suppression of inflammatory cytokine production by carbon monoxide involves the JNK pathway and AP-1. *J Biol Chem*, *278*, 36993–36998.

Nitti, M., Piras, S., Marinari, U. M., Moretta, L., Pronzato, M. A., & Furfaro, A. L. (2017). HO-1 induction in cancer progression: A matter of cell adaptation. *Antioxidants (Basel)*, *6*, E29.

Nowis, D., Bugajski, M., Winiarska, M., Jacek, B., Szokalska, A., Salwa, P., Issat, T., Was, H., Jozkowicz, A., Dulak, J., Stoklosa, T., & Golab, J. (2008). Zinc protoporphyrin IX, a heme oxygenase-1 inhibitor, demonstrates potent antitumor effects but is unable to potentiate antitumor effects of chemotherapeutics in mice. *BMC Cancer*, *8*, 197.

Park, B. S., Kim, H. W., Rhyu, I. J., Park, C., Yeo, S. G., Huh, Y., Jeong, N. Y., & Jung, J. (2015). Hydrogen sulfide is essential for Schwann cell responses to peripheral nerve injury. *J Neurochem*, *132*, 230–242.

Parkinson, D. B., Bhaskaran, A., Arthur-Farraj, P., Noon, L. A., Woodhoo, A., Lloyd, A. C., Wrabetz, M. L., Wrabetz, L.,

Behrens, A., Mirsky, R., & Jessen, K. R. (2008). c-Jun is a negative regulator of myelination. *J Cell Biol*, *181*, 625–637.

Platt, J. L., & Nath, K. A. (1998). Heme oxygenase: Protective gene or Trojan horse. *Nat Med*, *4*, 1364–1365.

Ryter, S. W., Alam, J., & Choi, A. M. (2006). Heme oxygenase-1/carbon monoxide: From basic science to therapeutic applications. *Physiol Rev*, *86*, 583–650.

Salis, C., Setton, C. P., Soto, E. F., & Pasquini, J. M. (2007). The mRNA of transferrin is expressed in Schwann cells during their maturation and after nerve injury. *Exp Neurol*, *207*, 85–94.

Schipper, H. M., Cissé, S., & Stopa, E. G. (1995). Expression of heme oxygenase-1 in the senescent and Alzheimer-diseased brain. *Ann Neurol*, *37*, 758–768.

Schipper, H. M., Liberman, A., & Stopa, E. G. (1998). Neural heme oxygenase-1 expression in idiopathic Parkinson's disease. *Exp Neurol*, *150*, 60–68.

Schipper, H. M., Song, W., Zukor, H., Hascalovici, J. R., & Zeligman, D. (2009). Heme oxygenase-1 and neurodegeneration: Expanding frontiers of engagement. *J Neurochem*, *110*, 469–485.

Schipper, H. M., & Song, W. (2015). A heme oxygenase-1 transducer model of degenerative and developmental brain disorders. *Int J Mol Sci*, *16*, 5400–5419.

Shin, E. J., Jeong, J. H., Chung, Y. H., Kim, W. K., Ko, K. H., Bach, J. H., Hong, J. S., Yoneda, Y., & Kim, H. C. (2011). Role of oxidative stress in epileptic seizures. *Neurochem Int*, *59*, 122–137.

Shin, Y. H., Lee, S. J., & Jung, J. (2012). Secretion of ATP from Schwann cells through lysosomal exocytosis during Wallerian degeneration. *Biochem Biophys Res Commun*, *429*, 163–167.

Valek, L., Kanngießer, M., Häussler, A., Agarwal, N., Lillig, C. H., & Tegeder, I. (2015). Redoxins in peripheral neurons after sciatic nerve injury. *Free Radic Biol Med*, *89*, 581–592.

Verma, A., Hirsch, D. J., Glatt, C. E., Ronnett, G. V., & Snyder, S. H. (1993). Carbon monoxide: A putative neural messenger. *Science*, *259*, 381–384. Erratum in: (1994), *Science, 263*, 15.

Vreman, H. J., Ekstrand, B. C., & Stevenson, D. K. (1993). Selection of metalloporphyrin heme oxygenase inhibitors based on potency and photoreactivity. *Pediatr Res*, *33*, 195–200.

Wagner, K. R., Hua, Y., de Courten-Myers, G. M., Broderick, J. P., Nishimura, R. N., Lu, S. Y., & Dwyer, B. E. (2000). Tin-mesoporphyrin, a potent heme oxygenase inhibitor, for treatment of intracerebral hemorrhage: In vivo and in vitro studies. *Cell Mol Biol (Noisy-le-grand)*, *46*, 597–608.

Xie, Y., Wang, Y., Zong, C., & Cheng, J. (2014). Transforming growth factor-Beta inhibits heme oxygenase-1 expression in lung fibroblast through nuclear factor-kappa-B-dependent pathway. *Pharmacology*, *93*, 185–192.

Yama, K., Sato, K., Murao, Y., Tatsunami, R., & Tampo, Y. (2016). Epalrestat upregulates heme oxygenase-1, superoxide dismutase, and catalase in cells of the nervous system. *Biol Pharm Bull*, *39*, 1523–1530.

Yang, D. P., Kim, J., Syed, N., Tung, Y. J., Bhaskaran, A., Mindos, T., Mirsky, R., Jessen, K. R., Maurel, P., Parkinson, D. B., & Kim, H. K. (2012). p38 MAPK activation promotes denervated Schwann cell phenotype and functions as a negative regulator of Schwann cell differentiation and myelination. *J Neurosci*, *32*, 7158–7168.

Yoon, J., Bang, S. H., Park, J. S., Chang, S. T., Kim, Y. H., & Min, J. (2011). Increased in vitro lysosomal function in oxidative stress-induced cell lines. *Appl Biochem Biotechnol*, *163*, 1002–1011.